CrystEngComm

PAPER

View Article Online
View Journal | View Issue

Cite this: *CrystEngComm*, 2018, **20**, 4849

The influence of the secondary building linker geometry on the photochromism of naphthalenediimide-based metal–organic frameworks†

Chen Fu, Hai-Yu Wang, Guo-Shuai Zhang, Li Li, Ya-Nan Sun, Jia-Wei Fu and Hong Zhang *

Three novel square grid metal–organic frameworks (MOFs) based on cadmium have been synthesized successfully by analogous solvothermal reactions where *N*,*N*′-di(4-pyridylacylamino)-1,4,5,8-naphthalenediimide (IsoNDI) as the predesigned ligand was reacted with three kinds of aromatic dicarboxylic acids as the secondary building linkers. The geometries of these secondary building linkers have an influence on the formation of photochromism-leading intermolecular interactions in the obtained crystal structures. Owing to the existence of an NH group in the adopted NDI-type ligand, N–H···O hydrogen bonds are observed between the IsoNDI ligands and neighbouring dicarboxyl groups in all the compounds. However, face-to-face π–π stacking interactions are only found in compound **1** and not in **2** and **3**, for the naphthalene ring possessing a larger π-plane in **1** is more likely to form interactions with the π-conjugated planar IsoNDI ligand. Meanwhile, lone pair–π interactions appear in compounds **2** and **3** but not in **1** because their close packing patterns have a tendency to generate such interactions between adjacent IsoNDI ligands. Moreover, all three compounds exhibit interesting reversible photochromic behaviors in the presence of photoinduced electron transfers through the above intermolecular interactions. Besides, photocontrolled luminescence properties have also been investigated showing a competitive relationship with photochromic behaviors.

Received 30th May 2018,
Accepted 12th July 2018

DOI: 10.1039/c8ce00892b

rsc.li/crystengcomm

Introduction

As a class of breakthrough materials, metal–organic frameworks (MOFs) have drawn much interest because of their structural diversification and real or potential applications in many fields, such as gas storage, catalysis, biological applications, and conductivity.[1] In the past decades, chemical researchers have tried constantly to functionalize MOFs by means of chemical modification and anchoring that are performed on organic linkers[2] for their desirable specific properties on resultant architectures. Photochromic materials, one type of functional material, have also attracted much attention for their considerable potential applications in smart windows, information storage, erasable copy papers, optical switches, photomechanics, solar energy conversion, photoprinting and so forth.[3] Photochromic materials generally exhibit interesting color changes in response to UV or visible photoirradiation, which can be also coupled with the variation of some physical and chemical behaviors.[4] Many families of organic and inorganic photochromic compounds have been discovered where organic species are the major starting materials for their functional groups can be modified easily.[5] Until now, a great deal of materials based on different photoactive organic groups have been studied deeply in which photochromism roughly results from photoinduced isomerization,[6] enol–keto tautomerism,[7] *trans–cis* isomerization[8] and free radical generation.[9] Obviously, to construct photochromic MOFs, one new-type of multifunctional material derived from the combination of the photochromic properties and porosity of MOFs,[10] photochromic organic compounds are necessary. 1,4,5,8-Naphthalenediimide derivatives (NDIs), a class of neutral, π-conjugated, planar, highly redox-active compounds possessing a substitution on the diimide nitrogen, are often considered as excellent candidates for organic photochromic compounds. Thanks to their electron-accepting property, they usually participate in photoinduced electron transfer and undergo single one-electron reduction leading to the formation

Institute of Polyoxometalate Chemistry, Department of Chemistry, Northeast Normal University, Changchun, Jilin 130024, PR China.
E-mail: hope20130122@163.com, zhangh@nenu.edu.cn

† Electronic supplementary information (ESI) available: Graphics (Fig. S1–S12) and tables (Tables S1 and S2). CCDC 1561714, 1577758 and 1579879. For ESI and crystallographic data in CIF or other electronic format see DOI: 10.1039/c8ce00892b

of NDI radicals.[11] Hence, the assembly of NDIs and electron-donor components is an effective approach to establish the electron transfer route. Inspired by the idea of crystal engineering and reticular chemistry based on the fact that predesigned organic ligands and secondary building linkers can build the desired frameworks for organic chromophores,[12] we envisaged that it should be suitable to select NDIs as the predesigned organic ligands and electron-rich aromatic dicarboxylic acids as the secondary building linkers to construct photochromic MOFs.

With the above consideration, we have synthesized three 2-D cadmium based MOFs where we combined one NDI-type organic ligand—*N*,*N*′-di(4-pyridylacylamino)-1,4,5,8-naphthalenediimide (IsoNDI) with three different aromatic dicarboxylic acids, 2,6-naphthalenedicarboxylic acid (2,6-H_2NDC) in **1**, isophthalic acid (*m*-H_2BDC) in **2** and terephthalic acid (*p*-H_2BDC) in **3** (Fig. 1). Interestingly, these compounds all possess reversible photochromic properties in the solid states exhibiting obvious color changes upon irradiation *via* a xenon lamp (300 W). Notably, the different geometries of the secondary building linkers have made a significant impact on the crystal structures, thus forming divergent supramolecular interactions. Therefore, N–H···O hydrogen bonds can be observed in all compounds because of the existence of an NH group in the IsoNDI ligand, which plays a positive role in the structural stability and dimensionality. Meanwhile, face-to-face π–π stacking and lone pair–π interactions as unconventional non-covalent interactions are found respectively in **1**, **2** and **3** acting as the leading pathways to support photoinduced electron transfers.

Experimental

Materials and methods

All materials were purchased commercially and used without further purification. IsoNDI was synthesized following a previously reported process.[13] Elemental analyses (C, H and N) were performed using a PerkinElmer 2400 CHN elemental analyzer. The infrared spectra were measured in the range of 400–4000 cm^{-1} using a Mattson Alpha-Centauri spectrometer with KBr pellets. The powder X-ray diffraction (PXRD) patterns were recorded using a RigakuDmax 2000 X-ray diffractometer with graphite monochromatized Cu Kα radiation (λ = 0.15418 nm) and 2θ ranging from 5° to 50° at room temperature. Thermogravimetric analyses (TGA) of the crystalline samples were performed using a PerkinElmer thermal analyzer under nitrogen at a heat rate of 10 °C min^{-1} in the range of 10–800 °C. UV-vis absorption studies were performed using a Cary 500 UV-vis-NIR spectrophotometer. Electron spin resonance (ESR) studies were carried out at X-band frequency (9.45 GHz) on a Bruker EMX spectrometer while fluorescence spectra were obtained using a FLSP920 fluorescence spectrometer.

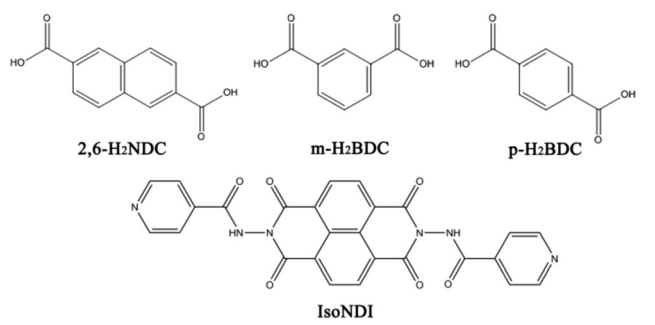

Fig. 1 The predesigned organic ligand and three secondary organic linkers employed in this study.

Preparation

Synthesis of [Cd(IsoNDI)(2,6-NDC)(H_2O)$_2$] (1). A mixture of IsoNDI (0.025 g, 0.05 mmol), 2,6-naphthalenedicarboxylic acid (2,6-H_2NDC) (0.0084 g, 0.05 mmol), $Cd(NO_3)\cdot 4H_2O$ (0.0308 g, 0.1 mmol), DMF (1 mL), MeOH (1 mL), and distilled water (2 mL) was sealed in a 25 mL Teflon-lined reactor autoclave and heated to 90 °C for 3 days. After cooling down to room temperature, the obtained orange single crystals of **1** were collected and washed with deionized water and then dried in air (18.53 mg, 43% yield based on IsoNDI). Anal. calcd (%) for $C_{38}H_{24}N_6O_{12}Cd$: C 52.53, H 2.76, N 9.67. Found: C 51.24, H 2.93, N 9.80. IR data (KBr, cm^{-1}): 3585 (w), 3476 (m), 3193 (w), 2955 (w), 2827 (w), 1680 (s), 1551 (s), 1359 (s), 1290 (s), 1244 (s), 1198 (m), 1130 (w), 1067 (m), 1025 (w), 1014 (m), 904 (m), 849 (m),755 (s), 697 (w), 579 (m), 489 (m), 459 (m), 404 (m).

Synthesis of [Cd(IsoNDI)(*m*-BDC)(DMF)] (2). A mixture of IsoNDI (0.025 g, 0.05 mmol), isophthalic acid (*m*-H_2BDC) (0.0085 g, 0.05 mmol), $Cd(NO_3)\cdot 4H_2O$ (0.0308 g, 0.1 mmol), DMF (4 mL), and H_2O (1 mL) was sealed in a 25 mL Teflon-lined reactor autoclave and heated to 95 °C for 4 days. After cooling down to room temperature, the obtained brownish yellow single crystals of **2** were collected and washed with DMF and then dried in air (13.78 mg, 37% yield based on IsoNDI). Anal. calcd (%) for $C_{37}H_{26}N_7O_{11}Cd$: C 51.86, H 3.03, N 11.45. Found: C 47.93, H 4.09, N 11.18. The difference is probably due to the presence of solvent molecules in the framework. Combined with TGA (Fig. S9†), there are approximately two DMF molecules by calculation. IR data (KBr, cm^{-1}): 3576 (w), 3504 (w), 3427 (s), 3171 (w), 2977 (w), 2831 (w), 1961 (w), 1734 (s), 1698 (s), 1604 (s), 1549 (s),1382 (s), 1297 (s), 1245 (s), 1201 (m), 1189 (w), 1133 (w), 984 (m), 905 (m), 852 (m), 745 (s), 678 (w), 581 (m), 515 (w).

Synthesis of [Cd_2(IsoNDI)$_2$(*p*-BDC)$_{0.5}$(MAC)$_2$] (MAC = methanoic acid) (3). A mixture of IsoNDI (0.025 g, 0.05 mmol), terephthalic acid (*p*-H_2BDC) (0.0085 g, 0.05 mmol), $Cd(NO_3)\cdot 4H_2O$ (0.0308 g, 0.1 mmol), DMF (4 mL), and H_2O (3 mL) was sealed in a 25 mL Teflon-lined reactor autoclave and heated to 95 °C for 4 days. After cooling down to room temperature, the obtained pale yellow single crystals of **3** were collected and washed with DMF and then dried in air (18.26 mg, 41% yield based on IsoNDI). Anal. calcd (%) for $C_{31}H_{17}N_6O_{10}Cd$: C 49.92, H 2.28, N 11.27. Found: C 48.54, H

2.55, N 11.46. IR data (KBr, cm^{-1}): 3590 (w), 3416 (w), 3176 (m), 3113 (w), 2999 (w), 2851 (w), 1965 (w), 1735 (s), 1662 (s), 1581 (s), 1385 (s), 1319 (s), 1242 (s), 1203 (m), 1138 (m), 1069 (m), 1033 (m), 1010 (m), 918 (m), 875 (m), 823 (m), 754 (s), 690 (m), 633 (w), 587 (s), 537 (m), 512 (w).

X-ray diffraction analysis

Crystal data for **1**, **2**, and **3** were collected using an Oxford Diffraction Gemini R Ultra diffractometer with graphite-monochromated Mo-Kα radiation (λ = 0.71073 Å) at 296 K. Absorption correction was applied by using the multiscan technique. The structures were solved and refined by full-matrix least-squares on F^2 using the program packages of Olex[14] and SHELXTL.[15] The thermal parameters of all the non-hydrogen atoms of the compounds were refined anisotropically, and the hydrogen atoms on the organic ligands were fixed at calculated positions. All of the crystal data and the structure refinements are summarized in Table S1, ESI.† The crystallographic data were deposited with the Cambridge Crystallographic Data Center (CCDC) as supplementary publication numbers CCDC 1561714, 1577758, and 1579879 for **1**, **2**, and **3**, respectively.

Results and discussion

Crystal structure of [Cd(IsoNDI)(2,6-NDC)(H_2O)$_2$] (1)

The single-crystal X-ray diffraction analysis indicates that compound **1** crystallizes in the monoclinic space group *C*2/*c*, and the asymmetric unit comprises one crystallographically independent Cd ion, half of one IsoNDI molecule, one 2,6-NDC^{2-} anion and one coordinated water molecule. As shown in Fig. S1a,† Cd(1) is octahedrally coordinated with two O atoms from two monodentate 2,6-NDC^{2-} anions (d_{Cd-O} = 2.218–2.254 Å), two N atoms from two electron-deficient IsoNDI tectons in a *trans* arrangement (d_{Cd-N} = 2.363–2.372 Å) and another two O atoms from two coordinated water molecules (d_{Cd-O} = 2.326–2.439 Å). Each of the Cd(II) cations is bridged with each other through monodentate μ^2-(2,6-NDC^{2-}) secondary linkers leading to an infinite 1-D horizontally shaped coordination polymer where every Cd cation is then capped at the top and bottom by two coordinated water molecules. Furthermore, the adjacent two 1-D coordination polymers connect with each other through the IsoNDI ligands forming a 2-D coordination framework (Fig. 2a). Interestingly, between the 2,6-NDC^{2-} linkers and the adjoined IsoNDI ligands, face-to-face π–π stacking interactions (3.351, 3.361 Å, Fig. 4a) and N–H···O hydrogen bonds (2.002 Å, Fig. 3a) are observed, which can not only stabilize crystal structure well but also generate a 3-D supramolecular network with one-dimensional channels (Fig. S2†). Also, inspection of the extended structure reveals that 2-D rectangular voids are formed (*ca.* 24.20 × 13.97 Å^2, Fig. 2a) and filled with solvent molecules, which is indeed supported by TGA showing that free water molecules are removed in the temperature range of 15–120 °C (calc. 2.4 wt%, Fig. S9a†). Most solvent molecules are disordered and all of them have been subtracted from the data using SQUEEZE during the refinement.

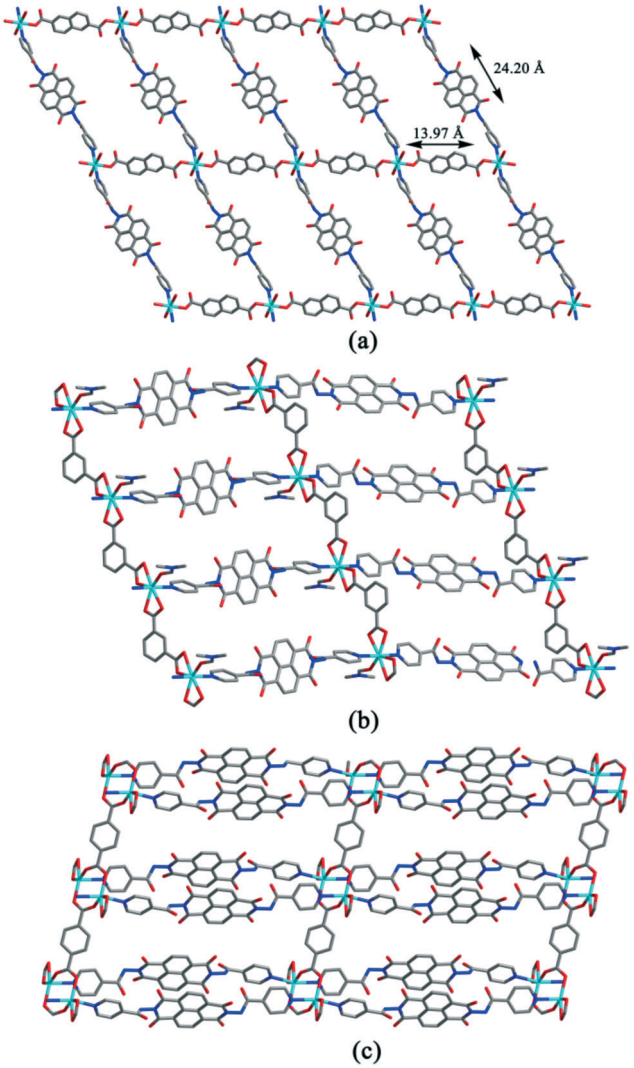

Fig. 2 (a) Orientation of **1** along the *a*- and *c*-axis. (b) Top view of the 2-D quadrate grid networks of **2**; (c) view of **3** along one orientation. All solvent molecules and hydrogen atoms were removed for clarity. Carbon atoms = grey, oxygen atoms = red, nitrogen atoms = blue, and cadmium atoms = turquoise.

Crystal structure of [Cd(IsoNDI)(*m*-BDC)(DMF)] (2)

Compound **2** crystallizes in the triclinic space group $P\bar{1}$, and the asymmetric unit contains one unique Cd ion, two half IsoNDI molecules, one *m*-BDC^{2-} anion and one DMF molecule. Cd(1) exhibits a slightly distorted pentagonal bipyramidal structure, coordinated with two N atoms from two IsoNDI ligands (d_{Cd-N} = 2.318–2.365 Å), four O atoms from two bidentate μ^2-(*m*-BDC^{2-}) linkers (d_{Cd-O} = 2.299–2.592 Å) and another O atom from one DMF molecule (d_{Cd-O} = 2.268 Å) (Fig. S1b†). As shown in Fig. 2b, the neighbouring Cd(II) centers are bridged by IsoNDI ligands forming an infinite 1-D coordination polymer where every two adjacent Cd(II) cations

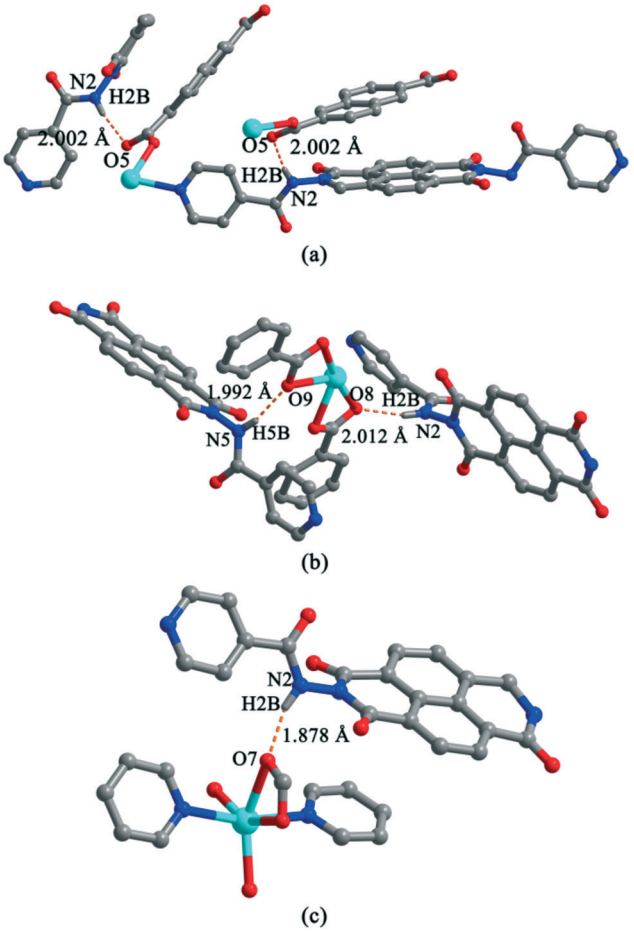

Fig. 3 N–H···O hydrogen bonds between IsoNDI ligands and neighbouring dicarboxyl groups in **1** (a), **2** (b) and **3** (c).

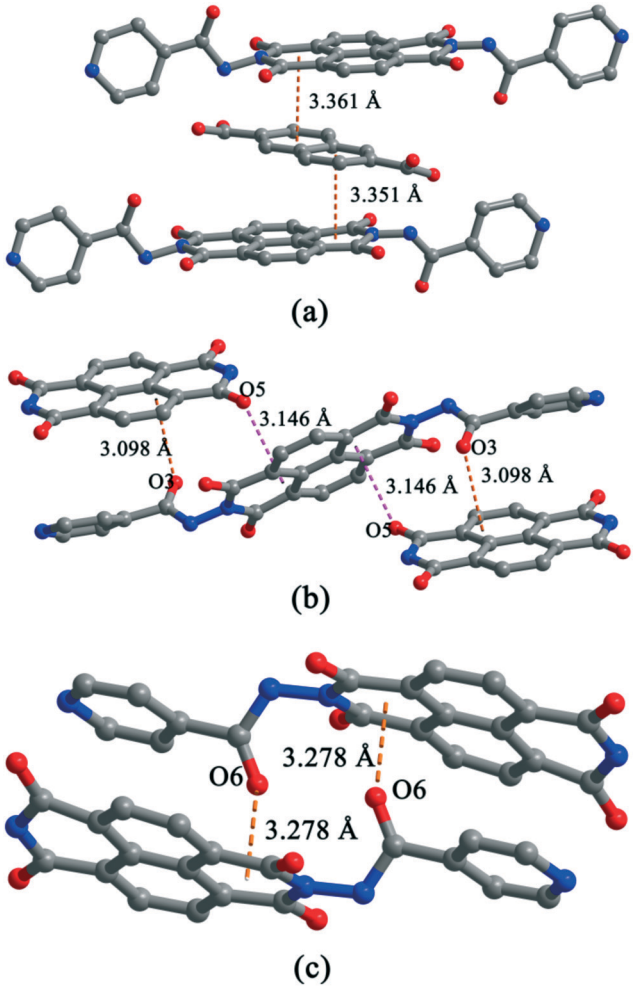

Fig. 4 Face-to-face π–π stacking interactions in **1** (a) and lone pair–π interactions in **2** (b) and **3** (c) between adjacent IsoNDI ligands.

are then capped by DMF molecules alternately at the top and bottom. Furthermore, parallel 1-D polymers are linked by bidentate μ^2-(*m*-BDC^{2-}) secondary linkers to produce a 2-D ladder-shaped framework in which IsoNDI ligands and μ^2-(*m*-BDC^{2-}) linkers can be considered vividly as the rungs and the handrails, respectively. Besides, intermolecular lone pair–π interactions between two neighboring IsoNDI ligands are observed (Fig. 4b) where the average O-ring distances are 3.098 Å and 3.146 Å, which can increase the strength of the coordination interaction between the metal cations and ligands[11] as well as generate a 3-D supramolecular network (Fig. S4†). Moreover, the network is further stabilized by the C–H···π interactions formed between the DMF molecules and neighbouring dicarboxyl groups or IsoNDI ligands ($d_{C-H\cdots\pi}$ = 3.458, 2.795, and 2.987 Å, Fig. S3†) and the N–H···O hydrogen bonds formed between the IsoNDI ligands and adjacent dicarboxyl groups ($d_{N-H\cdots O}$ = 1.992 and 2.012 Å, Fig. 3b).

Crystal structure of $[Cd_2(IsoNDI)_2(p\text{-}BDC)_{0.5}(MAC)_2]$ (3)

Compound **3** also crystallizes in the triclinic space group $P\bar{1}$, and the asymmetric unit consists of one Cd ion, one IsoNDI molecule, half of one *p*-BDC^{2-} anion and one $HCOO^-$ anion that resulted from the *in situ* decomposition of the DMF molecule.[16] As shown in Fig. S1c,† each center Cd cation is octahedrally coordinated with two N atoms from two IsoNDI ligands (d_{Cd-N} = 2.358–2.363 Å), two O atoms from one bidentate coordinated $HCOO^-$ anion (d_{Cd-O} = 2.380–2.446 Å) and another two O atoms from two monodentate *p*-BDC^{2-} linkers (d_{Cd-O} = 2.208–2.261 Å). The *p*-BDC^{2-} linker with four carboxylate O atoms in the μ^4 mode links with four Cd(II) cations to form two Cd_2 clusters with a Cd–Cd separation of 4.1238(7) Å. Each Cd_2 cluster can be considered as a node linked with four IsoNDI ligands leading to a pair of paralleled sheets, and the terminal coordinated $HCOO^-$ anions then point up and down the Cd_2 cluster sheets (Fig. 2c). Remarkably, the appearance of lone pair–π interactions ($d_{O\cdots\pi}$ = 3.278 and 3.543 Å, Fig. 4c and S5†) and N–H···O hydrogen bonds (d_{H-O} = 1.878 and 1.941 Å, Fig. 3c and S5†) in the 2-D sheets enriches the dimensionality of the crystal structure (Fig. S6†). Such a network in three dimensions is further stabilized by a kind of relatively weak π–π stacking interaction which is formed between the neighbouring center rings of the IsoNDI ligands with a distance of 3.762 Å (Fig. S5†). For

selected bond lengths and angles associated with the Cd cations of the three compounds see Table S2, ESI.†

Photochromism and mechanism

NDI-containing materials are usually photochromic because of the photoinduced electron transfer from the electron-rich group to the NDI ligand.[11] As we expected, compounds **1**–**3** all exhibit visible photochromic behaviors when they are irradiated upon with a xenon lamp (300 W) at room temperature in air. As shown in Fig. 5, orange crystals of **1** (**1a**) change into wine red after irradiation for 30 s and the coloration becomes saturated completely after irradiation for 10 min. The irradiated crystals (**1b**) are unstable relatively and can return to their original color in a dark room after one night at room temperature. The crystals of **2** can turn from brownish yellow (**2a**) into brownish black (**2b**), while the crystals of **3** can turn from pale yellow (**3a**) into purplish brown (**3b**) in 10 s and 3 min, respectively, and the discoloration saturation times are 10 min and 20 min. The photochromic products **2b** and **3b** are stable relatively and the original colors of the crystals can be restored in two weeks by dark treatment.

The unchanged PXRD patterns of the compounds during their reversible photochromism (Fig. S8†) indicate that the crystal structures still remain intact and further demonstrate that the origins of their photochromic properties are not photoinduced isomerization or photolysis. We speculated that such behaviors could be resulting from the IsoNDI free radical generation. Therefore, ESR and UV-vis absorption systematical characterization analysis methods were carried out in order to investigate the photochromic mechanism. As shown in Fig. 6, the time-dependent UV-vis spectra of **1**–**3** show that there are broad strong absorption bands in the range of 200–400 nm, which correspond to the typical π–π* and n–π* transitions occurring in the aromatic organic ligands.[17] However, in the range of 400–800 nm, different absorption results were obtained from the irradiated samples of **1**–**3**. In detail, there is a new absorption peak centered at 625 nm that appears in **1b**, five new absorption peaks at 475 nm, 540 nm, 610 nm, 702 nm, and 783 nm that occur in **2b**, while three broad absorption bands in the regions of 440–515 nm, 655–747 nm, 747–800 nm, an intrinsic absorption peak at 555 nm for being too sensitive to natural light and a new intense absorption peak at 602 nm arise in **3b**. What's more, the absorption intensity of these bands gradually increase when the irradiation time was prolonged. Based on previous reports,[18] the occurrence of these absorption bands may be attributed to the formation of IsoNDI radicals, and this potential possibility has been verified by the ESR study. As indicated in Fig. 7, the ESR study results show that there are no ESR signals before irradiation but single line signals are present with g = 2.0058 in **1b**, g = 2.0061 in **2b** and g = 2.0056 in **3b**, respectively, which are close to that of a free electron (g = 2.0023). Therefore, it is reasonable to believe that crystal photochromic properties are caused by the formation of IsoNDI radicals in photoinduced electron transfers. But what are the pathways to support these electron transfers?

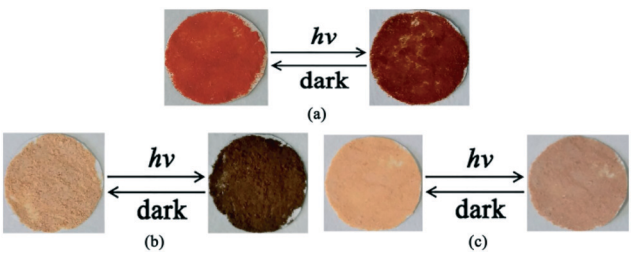

Fig. 5 Photographs of **1** (a), **2** (b) and **3** (c) before and after irradiation using a xenon lamp (300 W).

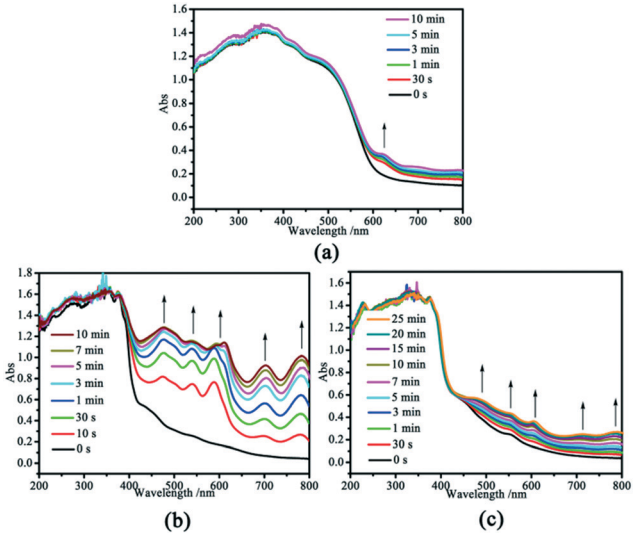

Fig. 6 Time-dependent UV-vis diffuse reflectance spectra of **1** (a), **2** (b) and **3** (c) *via* irradiation with a 300 W xenon lamp at room temperature in air.

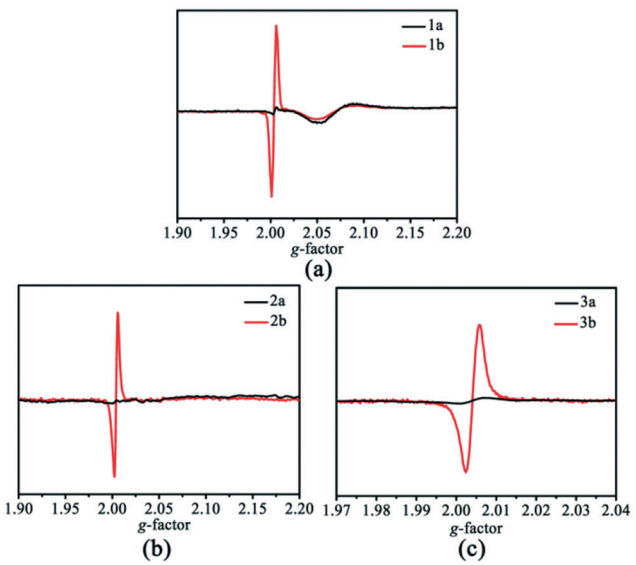

Fig. 7 ESR spectra of **1** (a), **2** (b) and **3** (c) before and after irradiation with a 300 W xenon lamp at room temperature in air.

As shown in Fig. 3, all compounds have N–H···O hydrogen bonds with H···O distances of 2.002, 1.992, and 1.878 Å for **1**, **2**, and **3**, respectively. The N–H···O hydrogen bonds have been demonstrated systematically that they are suitable for the so-called through-space electron transfer.[19] So it should be logically reasonable that the discoloration rate of **3** (1.878 Å) is greater than or close to those of **1** and **2** if their photoinduced electron transfers are supported by such N–H···O hydrogen bonds. However, it is actually the contrary that the photochromism of **3** is the weakest, distinctly. So, the N–H···O hydrogen bonds are not the key factor to the photochromism. In some cases of NDI derivatives,[20] π–π stacking interactions can affect the photochromic behaviors efficiently and play a crucial role in stabilizing the radicals of the NDIs. Luckily, face-to-face π–π stacking interactions formed between the centroid of an IsoNDI and benzene rings of an aromatic dicarboxylic acid with inter-ring shortest distances of 3.351 Å and 3.361 Å are found in **1** (Fig. 4a) but not in **2** and **3**, which may be attributed to the influence of the secondary building linker geometries on the spatial organization of the self-assembled materials; the naphthalene ring possessing a larger π-plane is more likely to form interactions with a π-conjugated planar IsoNDI ligand. In the electron transfer process, the 2,6-NDC^{2-} chromophoric linker itself as the donor component donates an electron to the IsoNDI ligand.

Although there are no π–π stacking interactions in **2** and **3**, the arrangements of close crystalline packing modes facilitate the appearance of intermolecular lone pair–π interactions between two neighbouring IsoNDI ligands, in which the shortest O-ring distances are 3.098 Å and 3.278 Å, respectively (Fig. 4b and c). Generally, the coordinated IsoNDI molecules in the crystal structure have a dual role: as electron acceptors (centroid rings) and electron donors (the oxygen atoms from the carbonyl groups) in the lone pair–π interactions. The previous study on a TauNDI-based photochromic coordination network by Liao *et al.*[21] has shown that similar lone pair–π interactions formed between adjacent TauNDI molecules have made a key effect on the photochromism. Therefore, we have reasons to believe that their photochromic behaviors are caused by such observed lone pair–π interactions. To further prove the mechanism, we have made IsoNDI free ligands irradiated under the same light conditions. As a result, the yellow samples changed into brown after irradiation for 10 minutes showing similar photochromic behaviour. As depicted in Fig. S11,† there exist two intrinsic broad absorption bands in the regions of 490–525 nm and 525–575 nm, two new broad absorption bands in the regions of 660–735 nm and 735–800 nm, and a new intense absorption peak at 607 nm in the UV-vis spectrum of the irradiated IsoNDI ligand, which suggests the formation of IsoNDI radicals during irradiation. According to the structural features of the IsoNDI ligand, the pathway that supports electron transfer can only be intermolecular lone pair–π interactions which are formed between oxygen atoms from carbonyl groups and electron-deficient centroid rings or pyridine rings. On the other hand, the contrastive analyses of absorption peak positions in **1b**, **2b**, **3b** and the irradiated IsoNDI ligand can also demonstrate that the causes for the photochromism of **2** and **3** are identical to that of the free IsoNDI ligand but different from that of **1**. Besides, the more sensitive photochromism of **2** compared to **3** results from exactly the stronger lone pair–π interactions (3.098 Å in **2** and 3.278 Å in **3**). Additionally, it is worth noting that lone pair–π interactions cooperating with the close packing patterns have strengthened the interaction between neighbouring IsoNDI ligands significantly to produce stable IsoNDI radicals with long-lived charge-separated states,[18] which can be supported by the longer decoloration times of **2** and **3**.

Luminescence properties

Photo-controlled luminescence properties are usually mentioned in the study of photochromic materials as another product of the electron transfer process. Compounds **1–3** all exhibit evident fluorescence quenching phenomena. As shown in Fig. 8, their fluorescent spectra indicate that there is a strong emission peak at 628 nm and a weak peak at 403 nm upon excitation at 380 nm of **1**, two emission peaks at 418 and 438 nm upon excitation at 375 nm of **2**, and three emission peaks at 534, 570 and 612 nm upon excitation at 390 nm of **3** at room temperature. Moreover, these emission peaks are gradually reduced upon irradiation, and almost totally quenched after being irradiated for 10, 5, and 20 minutes, respectively. The results illustrate that photochromism and photo-controlled luminescence can take place simultaneously and maintain a competitive relationship with each other in spite of the common origin of their photoinduced electron transfer. Similarly, the fluorescence intensity can be also restored when the irradiated samples recover their initial states by dark treatment. In addition, the luminescence properties of the IsoNDI free ligand have also been

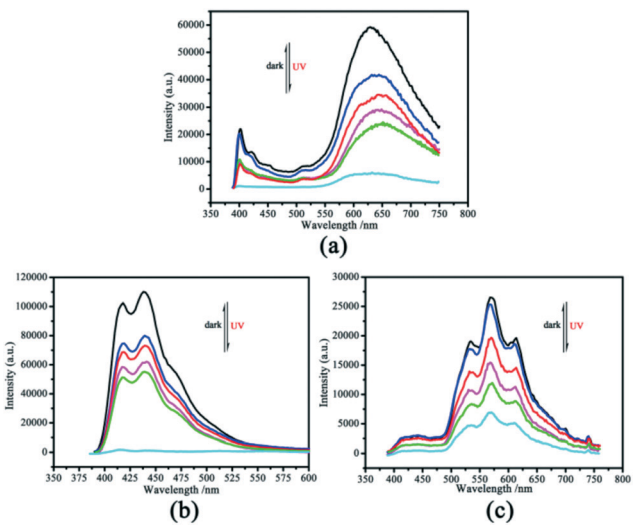

Fig. 8 Time-dependent photo-controlled fluorescence spectra of **1** (a), **2** (b) and **3** (c) upon irradiation (λ_{ex} = 380, 375 and 390 nm, respectively) at room temperature in air.

studied. As shown in Fig. S12,† there are three emission peaks at 519, 549 and 584 nm upon excitation at 380 nm in its fluorescent spectrum whose intensity can also be decreased upon irradiation. Furthermore, the fluorescent spectra of the IsoNDI ligand and **3** are similar, which indicates that the primary ligand-IsoNDI has a decisive influence on the emission of **3** particularly.

Conclusion

In summary, we have introduced the syntheses and structures of three naphthalenediimide-based MOFs containing different secondary building linkers. Interestingly, they exhibit various photochromism and photo-controlled luminescence phenomena upon irradiation using a xenon lamp (300 W), which mainly result from intermolecular π–π stacking and lone pair–π interactions. Besides, N–H···O hydrogen bonds are also generated between IsoNDI ligands and neighbouring carboxyl groups in the three compounds, which play a positive role in structural stability and dimensionality. This work has demonstrated factually the influence of the secondary building linker geometry on the framework structures showing the formation of different supramolecular interactions and further illustrated the impact of the above two kinds of non-covalent interactions on the photochromism of NDI-based materials, and we wish that this will provide valuable insight into designing new photochromic materials through such introduced supramolecular interactions.

Conflicts of interest

There are no conflicts to declare.

Acknowledgements

We gratefully acknowledge financial support from the NSF of China (21571032 and 21271038), the China High-Tech Development 863 program (2007AA03Z218) and the analysis and testing foundation of Northeast Normal University.

References

1 (*a*) J.-R. Li, J. Sculley and H.-C. Zhou, *Chem. Rev.*, 2012, **112**, 869; (*b*) K. Sumida, D. L. Rogow, J. A. Mason, T. M. McDonald, E. D. Bloch, Z. R. Herm, T. H. Bae and J.-R. Long, *Chem. Rev.*, 2012, **112**, 724; (*c*) F. K. Shieh, S.-C. Wang, C. I. Yen, C.-C. Wu, S. Dutta, L.-Y. Chou, J. V. Morabito, P. Hu, M. H. Hsu, C.-W. Wu and C. K. Tsung, *J. Am. Chem. Soc.*, 2015, **137**, 4276; (*d*) F. Lyu, Y. Zhang, R. N. Zare, J. Ge and Z. Liu, *Nano Lett.*, 2014, **14**, 5761; (*e*) L. Sun, M. G. Campbell and M. Dinca, *Angew. Chem., Int. Ed.*, 2016, **55**, 3566.

2 Z.-Q. Wang and S. M. Cohen, *Chem. Soc. Rev.*, 2009, **38**, 1315.

3 (*a*) C. Bechinger, S. Ferrere, A. Zaban and J. Sprague, *Nature*, 1996, **383**, 608; (*b*) S. Kawata and Y. Kawata, *Chem. Rev.*, 2000, **100**, 1777; (*c*) M.-S. Wang, G. Xu, Z.-J. Zhang and G.-C. Guo, *Chem. Commun.*, 2010, **46**, 361; (*d*) R. Pardo, M. Zayat and D. Levy, *Chem. Soc. Rev.*, 2011, **40**, 672; (*e*) B. Garai, A. Mallick and R. Banerjee, *Chem. Sci.*, 2016, **7**, 2195; (*f*) L. A. Vermeulen and M. E. Thompson, *Nature*, 1992, **358**, 656.

4 (*a*) M. Irie, T. Fukaminato, K. Matsuda and S. Kobatake, *Chem. Rev.*, 2014, **114**, 12174; (*b*) H. B. Laurent and H. Dürr, *Pure Appl. Chem.*, 2001, **73**, 639; (*c*) E. Hadjoudis and I. M. Mavridis, *Chem. Soc. Rev.*, 2004, **33**, 579; (*d*) K. Amimoto and T. Kawato, *J. Photochem. Photobiol., A*, 2005, **6**, 207.

5 (*a*) R. Exelby and R. Grinter, *Chem. Rev.*, 1965, **65**, 247; (*b*) M. Irie, *Chem. Rev.*, 2000, **100**, 1685; (*c*) Y. Yokoyama, *Chem. Rev.*, 2000, **100**, 1717; (*d*) Y. Kishimoto and J. Abe, *J. Am. Chem. Soc.*, 2009, **131**, 4227.

6 (*a*) M.-Q. Zhu, L. Zhu, J.-J. Han, W. WU, J. K. Hurst and A.-D.-Q. Li, *J. Am. Chem. Soc.*, 2006, **128**, 4303; (*b*) F.-Y. Lin and K. Morokuma, *J. Am. Chem. Soc.*, 2013, **135**, 10693.

7 E. Hadjoudis and I. M. Mavridis, *Chem. Soc. Rev.*, 2004, **33**, 579.

8 (*a*) R. Lyndon, K. Konstas, B. P. Ladewig, P. D. Southon, C. J. Kepert and M. R. Hill, *Angew. Chem., Int. Ed.*, 2013, **52**, 3695; (*b*) J. Park, D.-Q. Yuan, K. T. Pham, J.-R. Li, A. Yakovenko and H.-C. Zhou, *J. Am. Chem. Soc.*, 2012, **134**, 99.

9 (*a*) J.-K. Sun, L.-X. Cai, Y.-J. Chen, Z.-H. Li and J. Zhang, *Chem. Commun.*, 2011, **47**, 6870; (*b*) A. Kikuchi, F. Iwahori and J. Abe, *J. Am. Chem. Soc.*, 2004, **126**, 6526; (*c*) K. Shima, K. Mutoh, Y. Kobayashi and J. Abe, *J. Am. Chem. Soc.*, 2014, **136**, 3796.

10 (*a*) L. Han, L. Qin, L.-P. Xu, Y. Zhou, J.-L. Sun and X.-D. Zou, *Chem. Commun.*, 2013, **49**, 406; (*b*) M.-S. Wang, G.-C. Guo, W.-Q. Zou, W.-W. Zhou, Z.-J. Zhang, G. Xu and J.-S. Huang, *Angew. Chem., Int. Ed.*, 2008, **47**, 3565; (*c*) Q.-L. Zhu, T.-L. Sheng, R.-B. Fu, S.-M. Hu, L. Chen, C.-J. Shen, X. Ma and X.-T. Xu, *Chem. – Eur. J.*, 2011, **17**, 3358; (*d*) Z.-Y. Fu, Y. Chen, J. Zhang and S.-J. Liao, *J. Mater. Chem.*, 2011, **21**, 7895.

11 (*a*) S. V. Bhosale, C. H. Jani and S. J. Langford, *Chem. Soc. Rev.*, 2008, **37**, 331; (*b*) M. Pan, X.-M. Lin, G.-B. Li and C.-Y. Su, *Coord. Chem. Rev.*, 2011, **255**, 1921; (*c*) M. A. Kobaisi, K. Latham, A. M. Raynor and S. V. Bhosale, *Chem. Rev.*, 2016, **116**, 11685.

12 (*a*) L. Han, L.-P. Xu, L. Qin, W.-N. Zhao, X.-Z. Yan and L. Yu, *Cryst. Growth Des.*, 2013, **13**, 4260; (*b*) N. Sikdar, K. Jayaramulu, V. Kiran, K. V. Rao, S. Sampath, S. J. George and T. K. Maji, *Chem. – Eur. J.*, 2015, **21**, 11701.

13 S. Bhattacharjee, B. Maiti and S. Bhattacharya, *Nanoscale*, 2016, **8**, 11224.

14 O. V. Dolomanov, L. J. Bourhis, R. J. Gildea, J. A. K. Howard and H. Puschmann, *J. Appl. Crystallogr.*, 2009, **42**, 339.

15 G. Sheldrick, *Acta Crystallogr., Sect. A: Found. Crystallogr.*, 2008, **64**, 112.

16 (*a*) Y.-S. Liu, Y.-H. Luo, L. Li and H. Zhang, *Photochem. Photobiol. Sci.*, 2017, **16**, 753; (*b*) S.-T. Zheng, T. Wu, B. Irfanoglu, F. Zuo, P.-Y. Feng and X.-H. Bu, *Angew. Chem., Int. Ed.*, 2011, **50**, 8034.

17 (*a*) J.-Z. Liao, H.-L. Zhang, S.-S. Wang, J.-P. Yong, X.-Y. Wu,

R.-M. Yu and C.-Z. Lu, *Inorg. Chem.*, 2015, **54**, 4345; (*b*) J. Wang, S.-L. Li and X.-M. Zhang, *ACS Appl. Mater. Interfaces*, 2016, **8**, 24862; (*c*) J.-J. Liu, S.-B. Xia, Y.-L. Duan, T. Liu, F.-X. Cheng and C.-K. Sun, *Polymer*, 2018, **10**, 165.

18 (*a*) C. R. Wade, M. Li and M. Dincă, *Angew. Chem., Int. Ed.*, 2013, **52**, 13377; (*b*) B. Garai, A. Mallick and R. Banerjee, *Chem. Sci.*, 2016, **7**, 2195; (*c*) J.-Z. Liao, C. Wu, X.-Y. Wu, S.-Q. Deng and C.-Z. Lu, *Chem. Commun.*, 2016, **52**, 7394.

19 Z.-W. Chen, G. Lu, P.-X. Li, R.-G. Lin, L.-Z. Cai, M.-S. Wang and G.-C. Guo, *Cryst. Growth Des.*, 2014, **14**, 2527.

20 (*a*) A. Mallick, B. Garai, M. A. Addicoat, P. S. Petkov, T. Heine and R. Banerjee, *Chem. Sci.*, 2015, **6**, 1420; (*b*) B. Garai, A. Mallick and R. Banerjee, *Chem. Sci.*, 2016, **7**, 2195; (*c*) S. Guha and S. Saha, *J. Am. Chem. Soc.*, 2010, **132**, 17674; (*d*) J.-Z. Liao, C. Wu, X.-Y. Xu, S.-Q. Deng and C.-Z. Lu, *Chem. Commun.*, 2016, **52**, 7394; (*e*) B. D. McCarthy, E. R. Hontz, S. R. Yost, T. V. Voorhis and M. Dinca, *J. Phys. Chem. Lett.*, 2013, **4**, 453.

21 J.-Z. Liao, J.-F. Chang, L.-Y. Meng, H.-L. Zhang, S.-S. Wang and C.-Z. Lu, *Chem. Commun.*, 2017, **53**, 9701.

